In-Plane Shear Characterisation of Uni-Directionally Reinforced Thermoplastic Melts

S.P. Haanappel[*], R. ten Thije[†], U. Sachs[*], A.D. Rietman[**] and R. Akkerman[**,*]

[*]*Thermoplastic Composite Research Centre, University of Twente, Horst building, P.O. Box 217, 7500AE Enschede, the Netherlands, www.tprc.nl, s.p.haanappel@utwente.nl, u.sachs@utwente.nl*
[†]*Aniform Virtual Forming, Nieuwstraat 116, 7411 LP Deventer, the Netherlands, www.aniform.com, r.tenthije@aniform.com*
[**]*Faculty of Engineering Technology, Chair of Production Technology, University of Twente, Drienerlolaan 5, P.O. Box 217, 7500AE Enschede, the Netherlands, r.akkerman@utwente.nl, a.d.rietman@utwente.nl*

Abstract. Intra-ply shear is an important mechanism in hot stamp forming processes of UD fibre reinforced thermoplastic laminates. Various methods have been developed to characterise this shear mechanism, but measured properties may differ for several orders of magnitude. Therefore, an alternative method to characterise the longitudinal shearing viscosity is presented. Straight fibre reinforced thermoplastic bars with a rectangular cross section are subjected to torsional loadings. The specimens' response can be used to characterise the shear properties of the fibre reinforced polymer melt. Different geometries and clamping conditions were modelled to show the sensitivity of the measured viscosity. Based on this, experiments were performed with thick bars with a PEI-AS4 and PEEK-AS4 composition. Frequency sweeps were applied at different temperatures. All measurements showed a clear shear thinning behaviour, which can conveniently be described with a power law model.

Keywords: intra-ply shear, thermoplastic, melts, viscosity, uni-directional, laminate, rectangular bar, torsion, rheometer

INTRODUCTION

Simulation tools for the stamp forming process of uni-directional (UD) fibre reinforced thermoplastics aim to reduce the number of optimisation cycles during the development phase of a product. Constitutive models are needed to describe the occurring deformation mechanisms, such as intra-ply shear, ply-ply and tool-ply friction, and out-of-plane bending. These models subsequently require reliable material property data and corresponding characterisation methods.

The well accepted Ideal Fibre Reinforced Newtonian fluid Model (IFRM) can be utilised to describe the deformation behaviour of a UD fibre reinforced Newtonian polymer melt [1]. This continuum theory assumes incompressibility and fibre-inextensibility. The stress tensor is expressed as:

$$\sigma = -p\mathbf{I} + T\vec{a}\vec{a} + 2\eta_T\mathbf{D} + 2(\eta_L - \eta_T)(\vec{a}\vec{a}\cdot\mathbf{D} + \mathbf{D}\cdot\vec{a}\vec{a}), \tag{1}$$

in which p is a hydrostatic pressure, T represents an arbitrary fibre stress, $\vec{a}$ is a unit vector that represents the fibre direction, and $\mathbf{D}$ is the rate of deformation tensor. The parameters η_T and η_L represent the transverse and longitudinal shearing viscosity of the UD reinforced ply respectively, and are related to the shearing mechanisms of a fibre reinforced viscous fluid as discussed in [2, 3].

The published methods for intra-ply shear characterisation result in distinctly different material parameters, as was summarised clearly in [2]. For example, a difference of several orders of magnitude was found between plate-plate rheology and picture frame experiments. Stamp forming simulations in which the magnitude of these shearing properties was varied resulted in different predictions of process induced defects [4]. Therefore, the development of an alternative shear characterisation technique is desired. The method in this paper deals with a straight rectangular bar that is subjected to a torsional load. The material is assumed to be a fibre reinforced polymer melt. The applied torque and the resulting deformation of the bar are related by its shearing properties. Analyses in the next sections will clarify the relation between the longitudinal viscosity and the torsional loadings. Characterisation experiments will be performed with a standard rheometer in oscillatory mode. Oscillating loadings and the effect of clamping conditions will be studied. Two composite systems will be characterised to demonstrate the use of this technique.

TORSION OF RECTANGULAR BARS

Consider a torsionally loaded rectangular straight bar of length L, width w, and thickness t, as shown in figures 1a and 1b. Assume that an unknown material property G is uniform over the entire cross section of the bar and that both bar ends are free to deform. This implies that bulging of the cross section is uniform over the length of the bar. The unknown property G can be determined if the shear stress and the shear strain at an arbitrary point in the cross section are both known. If we choose a point where these quantities have a maximum, namely at ($y = 0$, $z = t/2$), it can be shown that [5]:

$$\tau_{\max} = M \frac{24}{\pi^2} \frac{1}{t^2 w} \left(1 - \frac{192}{\pi^5} \frac{t}{w} \sum_{n=1,3,5,\ldots}^{\infty} \frac{1}{n^5} \tanh\left(\frac{n\pi w}{2t} \right) \right)^{-1} \sum_{n=1,3,5,\ldots}^{\infty} \frac{1}{n^2} \left(1 - \cosh^{-1}\left(\frac{n\pi w}{2t} \right) \right), \tag{2}$$

$$\gamma_{\max} = \phi \frac{8}{\pi^2} \frac{t}{L} \sum_{n=1}^{\infty} \frac{(-1)^{n+1}}{(2n-1)^2} \left(1 - \cosh^{-1}\left(\frac{(2n-1)\pi w}{2t} \right) \right) \sin\left(\frac{(2n-1)\pi}{2} \right), \tag{3}$$

where only the σ_{xy} and γ_{xy} components contribute to these maxima. These relations imply that a measured torque M and rotation angle ϕ, can be related to a shear stress and its associated shear strain, respectively. The unknown material parameter G can now be determined as $G = \tau_{\max}/\gamma_{\max}$.

Now suppose that an oscillating rotation angle $\phi = \phi_0 \sin(\omega t)$ with angular frequency ω is applied to the straight bar in figure 1a. Then generally a torsional response of the form $M = M_0 \sin(\omega t + \delta)$ will be measured. The phase angle δ appears in case of materials with viscous properties. Using equations (2) and (3), the oscillating rotation angle and torsional response can be converted to an oscillating shear strain and shear stress with amplitudes $\gamma_{0,\max}$ and $\tau_{0,\max}$, respectively. Then the conventional dynamic shear modulus and apparent viscosity can be defined as:

$$G' = \frac{\tau_{0,\max}}{\gamma_{0,\max}} \cos\delta \qquad \eta' = \frac{1}{\omega} \frac{\tau_{0,\max}}{\gamma_{0,\max}} \sin\delta \tag{4}$$

Note that the material parameters are assumed to be uniform over the entire rectangular cross section, such that these relations are only valid for materials with linear elastic and/or shear rate independent viscous behaviour (Newtonian fluids).

Clamping Sensitivity

Imposing a torsional load requires clamps near both ends of the fibre reinforced straight rectangular bar to transfer the forces (figure 2a). As a worst case scenario, it is assumed that the clamping conditions imply a restriction of bulging near both bar ends. For this situation, it was shown in [3] that the total torque is mainly carried by the fibres. This results in an over-estimation of the longitudinal viscosity. The AniForm finite element package [6] was utilised to relate the deviation η'/η_L to the thickness t of the bar.

The IFRM model (1) was used to describe the material behaviour. A fibre stiffness of $E_f = 134$GPa was used. The longitudinal and transverse viscosities were assumed equal and dimensions of $L = 47$ and $w = 13$mm were used. A mesh with quadratic tetrahedrae was used to model the straight bar. Boundary conditions were applied as indicated in figure 1b. An oscillating rotation angle $\phi = \phi_0 \sin(\omega t)$ with $\phi_0 = 0.3^\circ$ was imposed by prescribing the DOFs of the upper surface in y- and z-direction, whereas these DOFs of the lower surface were all suppressed. Torsional responses were extracted from the solution and the apparent viscosity η' was determined by using equations (2)-(4).

Results for different thicknesses t and several angular frequencies ω are shown in figure 1c. The apparent viscosity deviates around two orders of magnitude from the longitudinal viscosity, for small thicknesses. This deviation reduces with increasing angular frequency. The deviation also reduces for an increasing thickness of the rectangular bar. Additionally, increasing the angular frequency shows a little effect on the deviation for an increasing thickness. The deviations are small for straight bars without the uni-directional reinforcement, as shown by the dashed line. Suppose that specimens with dimensions of $L = 47$, $w = 13$, and $t = 10$mm are used in practice. According to the plotted graphs in figure 1c, the measured apparent viscosity η' will at most deviate 25% from the actual longitudinal viscosity η_L.

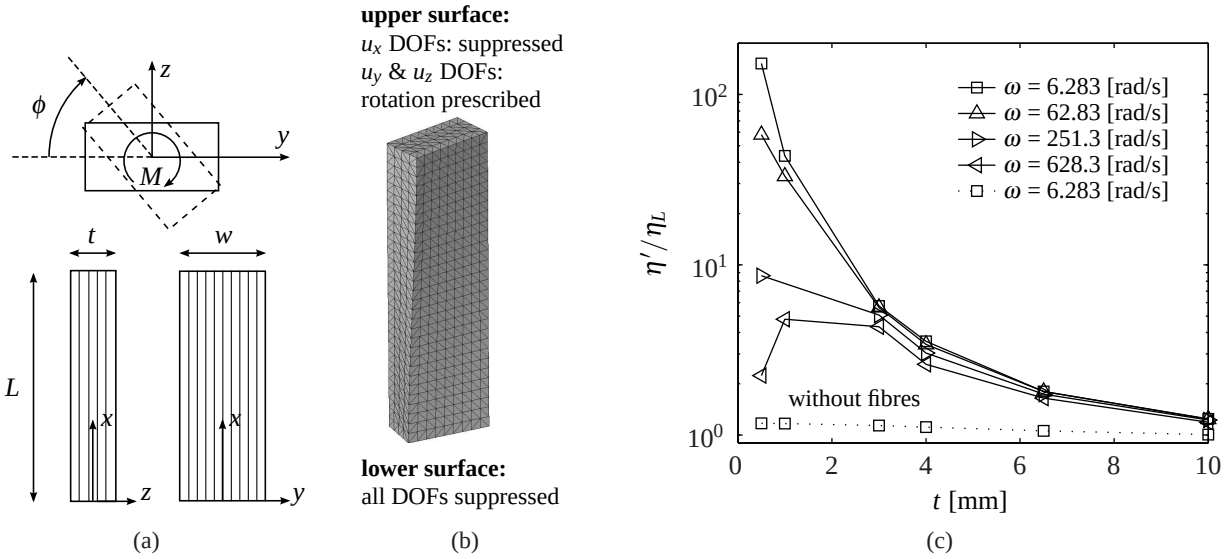

(a) (b) (c)

FIGURE 1. (a) Schematic representation of the UD reinforced straight bar. (b) Finite element mesh to model the straight bar. (c) Deviation of the apparent viscosity with the longitudinal viscosity as a function of the thickness of the straight bar.

RHEOLOGICAL EXPERIMENTS

Longitudinal viscosities were measured for two thermoplastic composite materials. CETEX Thermo-Lite® pre-preg materials from Ten Cate were used: a polyether ether ketone (PEEK) semi-crystalline polymer with an AS-4 carbon fibre reinforcement and a polyetherimide (PEI) amorphous polymer with an AS-4 carbon fibre reinforcement. Laminates were produced by stacking 80 equally orientated layers of the pre-preg material in a framed mould. Temperature and pressure cycles were applied, as instructed by the pre-preg manufacturer. Rectangular specimens as shown in figure 2b were subsequently cut from the laminate with a diamond wheel saw and dried in a vacuum oven at 80°C for at least 48 hours. Additional information can be found in Table 1.

Measurements were conducted by using an Anton Paar MC501 rheometer. Figure 2a shows a specimen that is mounted by a lower static fixture, and an upper movable fixture that transfers the torque from a controlled motor to the specimen. These standard fixtures (SRF12) for rectangular bars were slightly modified with two socket head cap screws. These screws transfer a clamping force to a guided plate that exerts a more evenly distributed clamping pressure on the specimen. Each specimen was clamped by tightening the screws gently until contact of the guided plate with the specimen was established. Since the specimens are tested at high temperatures and become viscous, high clamping pressures are avoided to prevent for squeeze flow mechanisms between the clamps. The clamping conditions will also change during the measurements due to thermal expansion of the specimen.

Five specimens per composite system were tested in a nitrogen environment at three distinct temperatures, within the range of stamp forming temperatures. Measurements were started, once the desired testing temperature and a steady state temperature distribution were reached (in approximately 10 minutes). In that case, temperature deviations of ≈10°C between the skin and points A and C in figure 2b, and ≈5°C between the skin and point B were observed. An 0.1N compressive normal force was controlled during heating to compensate the change in L due to thermal expansion. For each specimen and testing temperature, rotation angle sweeps with $0.05° \leq \phi_0 \leq 0.3°$ at an angular frequency of $\omega = 6.28$rad/s were performed. Since the apparent viscosity η' and the dynamical shear modulus G'

TABLE 1. Details of the carbon fibre reinforced thermoplastic specimens at room temperature.

					Polymer properties	
Thermoplastic -Fibre	t **[mm]**	w **[mm]**	L **[mm]**	**Fibre volume fraction**	**Glass transition temperature T_g[°C]**	**Melting temperature T_m[°C]**
PEI-AS4	10.7± 0.05	13.0± 0.1	47.1± 0.15	≈61.0%	215	-
PEEK-AS4	11.0± 0.05	13.0± 0.1	46.7± 0.15	≈59.3%	143	343

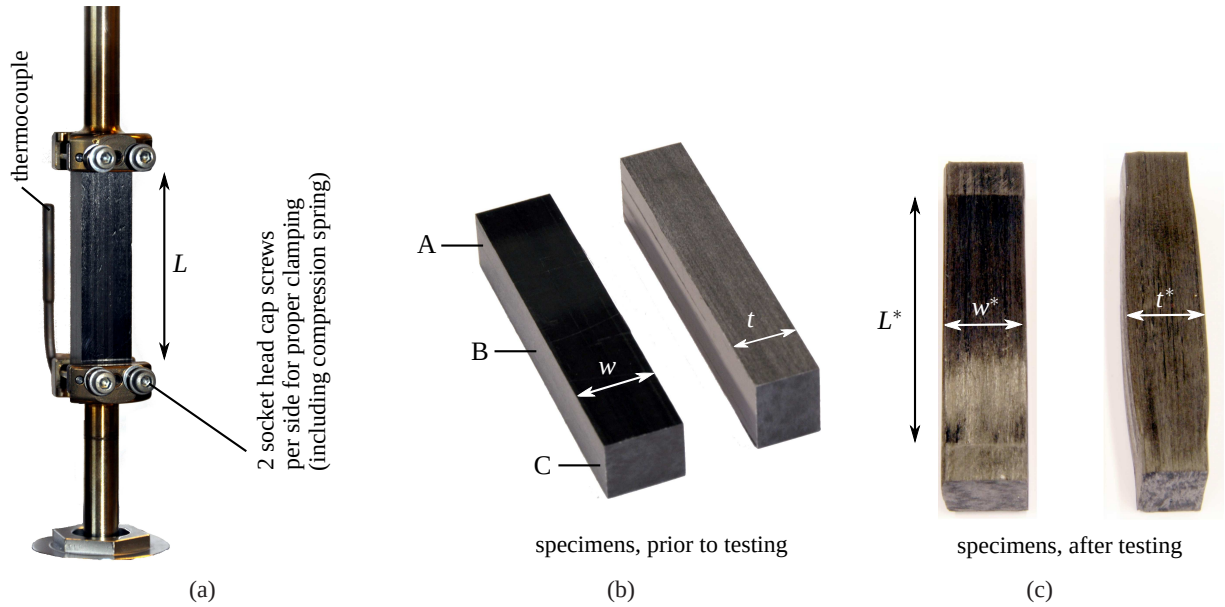

FIGURE 2. (a) Fixture with a mounted specimen. Length L indicates the length between the clamps, not the specimen's length. (b) Typical geometry of the specimens. Temperature deviations were evaluated within the specimen near points A, B, and C. (c) Deconsolidation processes result in change of the straight rectangular geometry. Typically, $w^* \approx 1.03w$, and $t^* \approx 1.15t$.

remained constant, subsequent frequency sweeps were conducted with $\phi_0 = 0.3°$ to gain sufficient resolution for torque amplitude readings.

Figure 3 shows the results of both composite systems. Initially, tests ① were performed in the lower temperature range. Thereafter, tests ② were performed in a medium temperature range, followed by tests ③ in a high temperature range. In the particular case of the semi-crystalline polymer PEEK, specimens were cooled down and tested ④ in the lower temperature range again. The results show the apparent viscosity according to equations (2)-(4). The solid lines represent upper bound viscosities for the specimen's original geometry with w and t, as shown in figure 2b. Deconsolidation processes that occur above T_g result in a change of geometry as show in figure 2c. The dashed lines in figure 3 assume a specimen geometry that is a straight bar with a rectangular cross section of w^* times t^*, resulting in a lower bound of η'. This geometry change gives rise to a 30% decrease of η' at most. Apart from this, the specimen's length L^* was continuously updated in these calculations. Note that all plotted apparent viscosities are at most 25% larger than the actual longitudinal viscosity, as concluded from the clamping sensitivity study.

All graphs show a decreasing apparent viscosity for increasing angular frequencies. This is generally referred to as shear thinning behaviour and can be described with a power law model. Comparing the low with the medium temperature range, a small decrease of η' can be observed for both composite systems. Nevertheless, this decrease is somewhat larger for the PEEK-AS4 system. A negligible change in viscosity is found by comparing the results of the medium with the high temperature range. Cooling down the PEEK-AS4 specimens to the initial testing temperature again ④, results in a lower viscosity than the initial measurements. It is likely that a semi-crystalline structure for tests ① was still present, whereas the crystallites were entirely molten for the tests ② and ③ at higher temperatures. These processes did not appear for the PEI-AS4 specimens due to the amorphous structure of the polymer.

DISCUSSION

Figure 3 shows the previously mentioned apparent viscosity η' of the reinforced systems, as well as the steady shear viscosity η of the neat thermoplastics [7]. The empirical Cox-Merz rule may be applied to translate the neat steady state viscosities to the magnitude of the complex dynamic viscosity, namely $\eta(\dot{\gamma}) \approx |\eta^*(\omega)|$. The magnitudes of both viscosities in figure 3 cannot be compared directly, because η' is the real part of η^*. However, $|\eta^*|$ was only slightly higher than η' for all cases such that a large difference between η_L and the neat viscosity η can still be concluded.

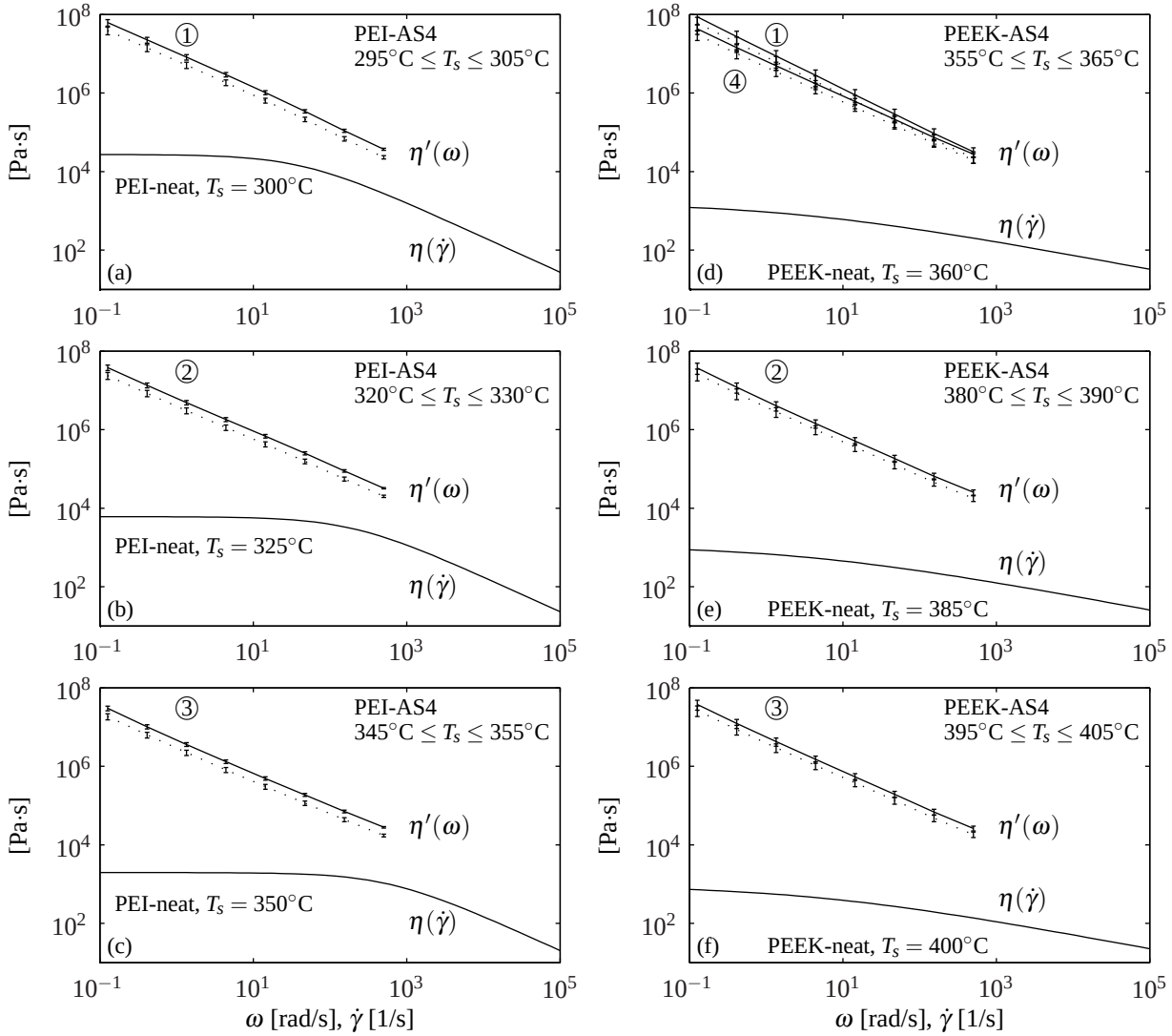

FIGURE 3. Apparent viscosity as a function of angular frequency for five PEI-AS4 specimens (left hand-side figures), and five PEEK-AS4 specimens (right hand-side figures). Rotation angle amplitudes of $\phi_0 = 0.3^\circ$ were used. Due to a temperature distribution T_s within the specimen, actual corrected temperatures are shown in the figures. The encircled numbering indicates the sequence of testing. Note that all plotted apparent viscosities η' are at most 25% larger than the actual longitudinal viscosity η_L, as concluded from the clamping sensitivity study. The lower solid lines show steady shear viscosities η of the neat thermoplastics [7].

It is also interesting to compare the slopes of $\eta'(\omega)$ and $\eta(\dot\gamma)$ in figure 3 (the experiments showed equal slopes for η' and $|\eta^*|$). Both composite systems show slopes of ≈ -0.9 for η'. For the associated range of shear rates, the neat resin viscosities η are within the Newtonian plateau or in the transition region to a viscosity with power law behaviour. The slope of $\eta(\dot\gamma)$ in the power law region is almost equal to the slope of $\eta'(\omega)$ for the PEI-AS4 system. This is clearly not the case for the PEEK-AS4 system.

For both composite systems, the slope of ≈ -0.9 for η' suggests almost rigid plastic behaviour. This implies a nearly constant (slighty increasing) shear stress and torque in the range of the plotted angular frequencies ω. The experiments showed a nearly constant torque (and G' from (4)) indeed. So far, it is hard to relate the characteristics of the neat thermoplastic properties to those of the reinforced systems, such as the Newtonian plateau. Additionally, there was no clear match between the slopes of the PEI-AS4 and PEEK-AS4 systems and their neat counterparts in the power law region.

It must be noted that all results are not corrected for the shear thinning behaviour. The viscosities were determined

with equations (2)-(4), which were based on uniform material properties over the entire rectangular cross section. Corrections need to be applied to account for the non-uniform material properties, such as the Weissenberg-Rabinowitch correction.

CONCLUSIONS

The IFRM model can be used to describe the constitutive behaviour of UD fibre reinforced thermoplastic melts. The material can be described with two characteristic viscosities. A novel characterisation technique to determine the longitudinal viscosity was presented in this paper. Applying oscillatory torsional loads to a straight bar with a rectangular cross section allows for its determination. Relations to determine this viscosity were shown. Uniform material properties over the entire specimen's cross section were assumed.

Finite element analyses were employed to investigate the deviation of the measured apparent viscosity, with respect to the longitudinal viscosity. A clamping situation that prevents both bar ends to bulge was modelled for different specimen geometries. Thicker rectangular bars show a rapidly decreasing deviation of the apparent viscosity. For the considered specimens, the measured apparent viscosity η' will deviate 25% at most from the actual longitudinal viscosity η_L.

Experiments were performed with PEI-AS4 and PEEK-AS4 specimens. Based on the clamping sensitivity study, thick rectangular specimens were produced and tested by means of a standard rheometer device. Five specimens per composite system were tested at three distinct temperatures. Small standard deviations were found, indicating the consistency of this characterisation method. Deconsolidation processes of the specimens occurred. Lower and upper bound viscosities were determined to account for this change in geometry. The lower bound shows 30% lower viscosities than the upper bound. Shear thinning mechanisms were clearly present for each situation and can be described with a power law viscosity model with relative ease.

The viscosity determination was based on the assumption of uniform material properties over the entire rectangular cross section of the specimen. Future work requires the correction of the experimental results to account for the shear rate dependent viscosity. Additionally, a translation from apparent to steady shear viscosities needs to be established. The possibility to translate the considered small strain to large strain deformations will also be assessed. Finally, the possibility to characterise the transverse viscosity will be considered by using differently oriented plies within the specimen.

ACKNOWLEDGMENTS

This project is funded by the Thermoplastic Composite Research Centre (TPRC). The support of the Region Twente and the Gelderland & Overijssel team for the TPRC, by means of the GO Programme EFRO 2007-2013, is gratefully acknowledged. Additionally, the author wants to thank the members of the technical advisory board of TPRC for the useful discussions and the supplied testing materials.

REFERENCES

1. T.G. Rogers, Rheological characterization of anisotropic materials. Composites, 20(1), 21-27, 1989.
2. P. Harrison, M.J. Clifford, In Design and manufacture of textile composites, Chapter 4, Rheological behaviour of pre-impregnated textiles. ed. A.C. Long, Woodhead Publishing Ltd., Cambridge, UK, 2005.
3. S.P. Haanappel, R.H.W. ten Thije, R. Akkerman, Constitutive modelling of UD reinforced thermoplastic laminates, Proceedings of the 10th International Conference on Flow Processes in Composite Materials, Centro Stefano Franscini, Monte Verità, Ascona, Switzerland, July 2010.
4. S.P. Haanappel, R.H.W. ten Thije, R. Akkerman., Forming predictions of UD reinforced thermoplastic laminates, Proceedings of the 14th European Conference on Composite Materials, Budapest, Hungary, June 2010.
5. S.P. Timoshenko, J.N. Goodier, Theory of Elasticity, 3rd ed., McGraw-Hill, 1970.
6. R. H. W. ten Thije, R. Akkerman, and J. Huétink, Large deformation simulation of anisotropic material using an updated Lagrangian finite element method, Computational Methods in Applied Mechanics and Engineering, 196:3141-3150, 2007.
7. Material Database from Autodesk Moldflow Insight 2011. Build 10243-001.